

Pan-keratin Immunostaining in Human Tumors: A Tissue Microarray Study of 15,940 Tumors

International Journal of Surgical Pathology
2023, Vol. 31(6) 927–938
© The Author(s) 2022



Article reuse guidelines:
sagepub.com/journals-permissions
DOI: 10.1177/10668969221117243
journals.sagepub.com/home/ijsp



Anne Menz, MD¹, Natalia Gorbokon, MD¹, Florian Viehweger, MD¹, Maximilian Lennartz, MD¹, Claudia Hube-Magg, MD¹, Lisa Hornsteiner, MD¹, Martina Kluth, MD¹, Cosima Völkel, MD¹, Andreas M. Luebke, MD¹, Christoph Fraune, MD¹, Ria Uhlig, MD¹, Sarah Minner, MD¹, David Dum, MD¹, Doris Höflmayer, MD¹, Guido Sauter, MD¹, Ronald Simon, MD¹ , Eike Burandt, MD¹ , Till S. Clauditz, MD¹, Patrick Lebok, MD¹, Frank Jacobsen, MD¹, Stefan Steurer, MD¹, Till Krech, MD², Andreas H. Marx, MD³, and Christian Bernreuther, MD¹

Abstract

To evaluate the efficiency of pan-keratin immunostaining, tissue microarrays of 13,501 tumor samples from 121 different tumor types and subtypes as well as 608 samples of 76 different normal tissue types were analyzed by immunohistochemistry. In normal tissues, strong pan-keratin immunostaining was seen in epithelial cells. Staining intensity was lower in hepatocytes, islets of Langerhans, and pneumocytes but markedly reduced in the adrenal cortex. Pan-keratin was positive in ≥98% of samples in 62 (83%) of 75 epithelial tumor entities, including almost all adenocarcinomas, squamous cell and urothelial carcinomas. Only 17 of 121 tumor entities (13%) had a pan-keratin positivity rate between 25% and 98%, including tumors with mixed differentiation, endocrine/neuroendocrine tumors, renal cell carcinomas, adrenocortical tumors, and particularly poorly differentiated carcinoma subtypes. The 15 entities with pan-keratin positivity in 0.9%-25% were mostly of mesenchymal origin. Reduced/absent pan-keratin immunostaining was associated with high UICC stage ($p = 0.0001$), high Thoenes grade ($p = 0.0183$), high Fuhrman grade ($p = 0.0049$), advanced tumor stage ($p < 0.0001$) and lymph node metastasis ($p = 0.0114$) in clear cell renal cell carcinoma, advanced pT stage ($p = 0.0007$) in papillary renal cell carcinoma, and with advanced stage ($p = 0.0023$), high grade ($p = 0.0005$) as well as loss of ER and PR expression (each $p < 0.0001$) in invasive breast carcinoma of no special type (NST). In summary, pan-keratin can consistently be detected in the vast majority of epithelial tumors, although pan-keratin can be negative a fraction of renal cell, adrenocortical and neuroendocrine neoplasms. The data also link reduced pan-keratin immunostaining to unfavorable tumor phenotype in epithelial neoplasms.

Keywords

pan-cytokeratin, pan-keratin, tissue microarray, immunohistochemistry, cancer

Introduction

Pan-keratin antibodies are mixtures of two or several antibodies that detect multiple low and high molecular weight keratins. These antibody cocktails have been designed to immunohistochemically detect all epithelial cell types irrespective of their tissues of origin with one single diagnostic tool. In surgical pathology they are typically employed to document the epithelial origin of neoplastic or non-neoplastic tissue or for detection of small metastases in lymph nodes. There are, however, limitations to the concept that pan-keratin antibodies stain all epithelial tumors and that non-epithelial tissues are “keratin negative”. For a large variety of different epithelial tumors,

pan-keratin negative tumors have been described^{1–6} and “keratin positive” mesenchymal tumors have also been reported across various mesenchymal tumor entities.^{7–12} The frequencies reported for pan-keratin negative

¹Institute of Pathology, University Medical Center Hamburg-Eppendorf, Hamburg, Germany

²Institute of Pathology, Clinical Center Osnabrück, Osnabrück, Germany

³Department of Pathology, Academic Hospital Fürth, Fürth Germany

Corresponding Author:

Prof Dr Ronald Simon, Institute of Pathology, University Medical Center Hamburg-Eppendorf, Martinistra. 52, 20246 Hamburg, Germany.
Email: R.Simon@uke.de

carcinomas and pan-keratin positive non-epithelial tumors varies considerably in the literature, however. For example, pan-keratin positivity has been described in 15% to 45% of hepatocellular carcinoma carcinomas,^{3,5} 0% to 95% of adrenocortical carcinomas,^{2,13,14} 33% to 100% of clear cell^{15,16} and 73% to 100% of papillary renal cell carcinomas,^{17,18} 20% to 78% of angiosarcomas,^{19,20} and 17% to 100% of leiomyosarcomas.^{21,22} These conflicting data may be caused by the use of different antibodies, immunostaining protocols, and criteria to determine “positivity” in these studies.

To generate a comprehensive dataset on the prevalence of pan-keratin positivity in epithelial and non-epithelial neoplasms, a set of tissue microarray (TMAs) was analyzed in this study that contained more than 15,500 tumor tissue samples from 121 different tumor types and subtypes as well as 76 different non-neoplastic tissue types.

Materials and Methods

Tissue Microarrays (TMAs). Our normal tissue TMA was composed of 8 samples from 8 different donors for each of 76 different normal tissue types (608 samples on one slide). The tumor TMAs contained a total of 15,940 primary tumors from 121 tumor types and subtypes. The composition of normal and tumor TMAs is described in the results section. Detailed histopathological and molecular data as well as clinical-follow up data were obtained from 1157 kidney and 1475 breast cancer patients. The median follow-up time was 39 months for kidney cancer (range 1-250) and 43 months for breast cancer patients (range 1-88). All samples were retrieved from the archives of the Institutes of Pathology, University Hospital of Hamburg, Germany, the Institute of Pathology, Clinical Center Osnabrueck, Germany, and Department of Pathology, Academic Hospital Fuerth, Germany. Tissues were fixed in 4% buffered formalin and then embedded in paraffin. The TMA manufacturing process was described earlier in detail.^{23,24} In brief, one tissue spot (diameter: 0.6 mm) was transmitted from a representative tumor containing donor block into an empty recipient paraffin block. The use of archived remnants of diagnostic tissues for TMA manufacturing, their analysis for research purposes, and use of patient data were according to local laws (HmbKHG, §12) and analysis had been approved by the local ethics committee (Ethics commission Hamburg, WF-049/09). All work has been carried out in compliance with the Helsinki Declaration.

Immunohistochemistry. Freshly cut TMA sections were immunostained on one day and in one experiment. Slides were deparaffinized and exposed to heat-induced antigen retrieval for 5 min in an autoclave at 121°C in a pH 9.0 buffer. The pan-cytokeratin antibody pan-keratin (recombinant rabbit, MSVA-000R, MS Validated Antibodies, GmbH, Hamburg, Germany) was applied at

37 °C for 60 min at a dilution of 1:150. Bound antibody was then visualized using the EnVision Kit (Agilent, CA, USA; #K5007) according to the manufacturer's directions. For tumor tissues, the percentage of positive neoplastic cells was estimated, and the staining intensity was semi-quantitatively recorded (0, 1 +, 2 +, 3 +). For statistical analyses, the staining results were categorized into four groups. Tumors without any staining were considered negative. Tumors with 1 + staining intensity in ≤70% of cells



Figure 1. Pan-keratin immunostaining of normal tissues. The panels show a strong pan-keratin positivity of epithelial cells of the stomach (A), the urothelium of the urinary bladder (B), and the squamous epithelium of the oral cavity (C). In the pancreas, acinar cells show a strong staining while cells of islets of Langerhans stain only weakly (D). In the liver pan-keratin staining is variable (weak to moderate) in hepatocytes but strong in bile ducts (E). In the adrenal gland, only a subset of cortical cells shows a weak staining (F). In the myometrium, groups of spindle-shaped pan-keratin positive cells are found (G). In lymph nodes, a delicate fibrillar staining caused by fibroblastic reticulum cells occurs mainly in the interfollicular area (H).

Table 1. Pan-Keratin Immunostaining in Human Tumors.

	Tumor entity	on TMA (n)	Pan-keratin immunostaining result				
			analyzable (n)	neg. (%)	weak (%)	mod. (%)	strong (%)
Tumors of the skin	Basal cell carcinoma	88	82	0.0	0.0	0.0	100.0
	Benign nevus	29	25	100.0	0.0	0.0	0.0
	Squamous cell carcinoma of the skin	90	88	0.0	1.1	0.0	98.9
	Malignant melanoma	48	43	93.0	0.0	4.7	2.3
	Merkel cell carcinoma	46	43	0.0	2.3	11.6	86.0
Tumors of the head and neck	Squamous cell carcinoma of the larynx	110	104	0.0	0.0	1.9	98.1
	Squamous cell carcinoma of the pharynx	60	58	0.0	0.0	0.0	100.0
	Oral squamous cell carcinoma (floor of the mouth)	130	125	0.8	0.8	0.0	98.4
	Pleomorphic adenoma of the parotid gland	50	35	0.0	0.0	8.6	91.4
	Warthin tumor of the parotid gland	49	45	0.0	0.0	0.0	100.0
Tumors of the lung, pleura and thymus	Basal cell adenoma of the salivary gland	15	15	0.0	0.0	0.0	100.0
	Adenocarcinoma of the lung	246	176	0.0	0.0	0.0	100.0
	Squamous cell carcinoma of the lung	130	73	0.0	0.0	2.7	97.3
	Small cell carcinoma of the lung	20	15	6.7	0.0	0.0	93.3
	Mesothelioma, epithelial	39	29	0.0	0.0	3.4	96.6
Tumors of the female genital tract	Mesothelioma, other types	76	63	3.2	0.0	1.6	95.2
	Thymoma	29	28	0.0	0.0	3.6	96.4
	Squamous cell carcinoma of the vagina	78	73	0.0	0.0	1.4	98.6
	Squamous cell carcinoma of the vulva	130	124	0.0	0.0	0.0	100.0
	Squamous cell carcinoma of the cervix	130	126	0.0	0.0	0.0	100.0
Tumors of the breast	Endometrioid endometrial carcinoma	236	220	0.9	0.5	0.9	97.7
	Endometrial serous carcinoma	82	70	1.4	0.0	2.9	95.7
	Carcinosarcoma of the uterus	48	44	15.9	2.3	2.3	79.5
	Endometrial carcinoma, high grade, G3	13	12	25.0	0.0	0.0	75.0
	Endometrial clear cell carcinoma	8	8	0.0	0.0	0.0	100.0
	Endometrioid carcinoma of the ovary	110	102	0.0	0.0	0.0	100.0
	Serous carcinoma of the ovary	559	509	0.4	0.2	0.6	98.8
	Mucinous carcinoma of the ovary	96	77	0.0	0.0	0.0	100.0
	Clear cell carcinoma of the ovary	50	45	0.0	0.0	2.2	97.8
	Carcinosarcoma of the ovary	47	39	15.4	5.1	0.0	79.5
Tumors of the digestive system	Brenner tumor	9	9	0.0	0.0	0.0	100.0
	Invasive breast carcinoma of no special type	1391	1152	0.3	0.6	1.0	98.1
	Lobular carcinoma of the breast	294	241	0.0	0.0	0.0	100.0
	Medullary carcinoma of the breast	26	26	0.0	0.0	0.0	100.0
	Tubular carcinoma of the breast	27	21	0.0	0.0	0.0	100.0
	Mucinous carcinoma of the breast	58	44	0.0	0.0	0.0	100.0
	Phyllodes tumor of the breast	50	43	0.0	0.0	0.0	100.0
	Adenomatous polyp, low-grade dysplasia	50	50	0.0	0.0	0.0	100.0
	Adenomatous polyp, high-grade dysplasia	50	46	0.0	0.0	0.0	100.0
	Adenocarcinoma of the colon	1932	1417	0.0	0.0	0.0	100.0
	Adenocarcinoma of the small intestine	10	7	14.3	0.0	0.0	85.7
	Gastric adenocarcinoma, diffuse type	226	158	0.0	0.0	0.6	99.4
	Gastric adenocarcinoma, intestinal type	224	162	1.2	0.0	0.0	98.8
	Gastric adenocarcinoma, mixed type	62	59	0.0	0.0	0.0	100.0
	Adenocarcinoma of the esophagus	133	77	0.0	0.0	1.3	98.7
	Squamous cell carcinoma of the esophagus	124	71	0.0	1.4	1.4	97.2
	Squamous cell carcinoma of the anal canal	91	87	0.0	0.0	0.0	100.0

(continued)

Table 1. (continued).

	Tumor entity	on TMA (n)	Pan-keratin immunostaining result			
			analyzable (n)	neg. (%)	weak (%)	mod. (%)
Tumors of the urinary system	Cholangiocarcinoma	114	106	0.0	0.0	0.0
	Hepatocellular carcinoma	50	50	0.0	10.0	12.0
	Ductal adenocarcinoma of the pancreas	662	551	0.2	0.0	0.4
	Pancreatic/Ampullary adenocarcinoma	119	84	0.0	0.0	0.0
	Acinar cell carcinoma of the pancreas	15	14	0.0	0.0	0.0
	Gastrointestinal stromal tumor (GIST)	50	47	95.7	0.0	2.1
	Non-invasive papillary urothelial carcinoma, pTa G2 low grade	177	147	0.0	0.0	0.0
	Non-invasive papillary urothelial carcinoma, pTa G2 high grade	141	122	0.0	0.0	0.0
	Non-invasive papillary urothelial carcinoma, pTa G3	187	118	0.0	0.0	2.5
	Urothelial carcinoma, pT2-4 G3	1207	862	0.9	0.3	0.9
	Small cell neuroendocrine carcinoma of the bladder	18	18	27.8	16.7	0.0
	Sarcomatoid urothelial carcinoma	25	21	23.8	4.8	4.8
Tumors of the male genital organs	Clear cell renal cell carcinoma	858	791	8.0	18.6	19.5
	Papillary renal cell carcinoma	255	236	0.8	1.3	1.7
	Clear cell (tubulo) papillary renal cell carcinoma	21	21	0.0	4.8	4.8
	Chromophobe renal cell carcinoma	131	126	0.8	0.0	0.0
	Oncocytoma	177	168	1.2	0.6	1.2
	Adenocarcinoma of the prostate, Gleason 3 + 3	83	83	0.0	0.0	0.0
	Adenocarcinoma of the prostate, Gleason 4 + 4	80	78	0.0	0.0	0.0
	Adenocarcinoma of the prostate, Gleason 5 + 5	85	85	0.0	0.0	0.0
	Adenocarcinoma of the prostate (recurrence)	261	252	0.0	0.0	2.0
	Small cell neuroendocrine carcinoma of the prostate	17	15	6.7	0.0	0.0
Tumors of endocrine organs	Seminoma	621	584	77.1	17.1	4.5
	Embryonal carcinoma of the testis	50	46	0.0	0.0	4.3
	Yolk sac tumor	50	42	0.0	0.0	4.8
	Teratoma	50	24	0.0	0.0	0.0
	Squamous cell carcinoma of the penis	80	78	0.0	0.0	0.0
	Adenoma of the thyroid gland	114	106	0.0	0.0	0.0
	Papillary thyroid carcinoma	392	366	0.0	0.3	0.0
	Follicular thyroid carcinoma	158	152	0.0	0.0	0.0
	Medullary thyroid carcinoma	107	103	0.0	0.0	0.0
	Anaplastic thyroid carcinoma	45	36	19.4	13.9	13.9
	Adrenal cortical adenoma	50	46	60.9	13.0	15.2
	Adrenal cortical carcinoma	26	25	52.0	16.0	4.0
	Phaeochromocytoma	50	47	100.0	0.0	0.0
	Appendix, neuroendocrine tumor	22	16	0.0	0.0	6.3
	Colorectal, neuroendocrine tumor	11	11	0.0	0.0	0.0
Tumors of	Ileum, neuroendocrine tumor	49	46	0.0	0.0	0.0
	Lung, neuroendocrine tumor	19	18	5.6	0.0	0.0
	Pancreas, neuroendocrine tumor	98	91	0.0	1.1	4.4
	Colorectal, neuroendocrine carcinoma	12	10	20.0	0.0	0.0
	Gallbladder, neuroendocrine carcinoma	4	4	50.0	0.0	0.0
	Pancreas, neuroendocrine carcinoma	14	14	0.0	7.1	0.0
	Hodgkin Lymphoma	103	103	99.0	1.0	0.0

(continued)

Table 1. (continued).

	Tumor entity	on TMA (n)	Pan-keratin immunostaining result				
			analyzable (n)	neg. (%)	weak (%)	mod. (%)	strong (%)
haemopoietic and lymphoid tissues	Non-Hodgkin Lymphoma	62	61	100.0	0.0	0.0	0.0
	Small lymphocytic lymphoma, B-cell type	50	50	100.0	0.0	0.0	0.0
	Diffuse large B cell lymphoma	114	114	100.0	0.0	0.0	0.0
	Follicular lymphoma	88	88	100.0	0.0	0.0	0.0
	T-cell Non Hodgkin lymphoma	24	24	100.0	0.0	0.0	0.0
	Mantle cell lymphoma	18	18	100.0	0.0	0.0	0.0
	Marginal zone lymphoma	16	16	100.0	0.0	0.0	0.0
	Diffuse large B-cell lymphoma in the testis	16	16	100.0	0.0	0.0	0.0
	Burkitt lymphoma	5	3	100.0	0.0	0.0	0.0
Tumors of soft tissue and bone	Tenosynovial giant cell tumor	45	45	100.0	0.0	0.0	0.0
	Granular cell tumor	53	46	100.0	0.0	0.0	0.0
	Leiomyoma	50	44	86.4	13.6	0.0	0.0
	Leiomyosarcoma	87	85	81.2	12.9	4.7	1.2
	Liposarcoma	132	116	94.8	3.4	1.7	0.0
	Malignant peripheral nerve sheath tumor	13	13	100.0	0.0	0.0	0.0
	Myofibrosarcoma	26	26	100.0	0.0	0.0	0.0
	Angiosarcoma	73	65	75.4	9.2	3.1	12.3
	Angiomyolipoma	91	86	88.4	10.5	1.2	0.0
	Dermatofibrosarcoma protuberans	21	17	94.1	5.9	0.0	0.0
	Ganglioneuroma	14	12	100.0	0.0	0.0	0.0
	Kaposi sarcoma	8	5	100.0	0.0	0.0	0.0
	Neurofibroma	117	107	99.1	0.9	0.0	0.0
	Sarcoma, not otherwise specified (NOS)	75	73	90.4	4.1	1.4	4.1
	Paraganglioma	41	41	100.0	0.0	0.0	0.0
	Ewing Sarcoma	23	15	100.0	0.0	0.0	0.0
	Rhabdomyosarcoma	7	7	71.4	28.6	0.0	0.0
	Schwannoma	121	117	96.6	3.4	0.0	0.0
	Synovial sarcoma	12	11	81.8	18.2	0.0	0.0
	Osteosarcoma	43	33	87.9	0.0	9.1	3.0
	Chondrosarcoma	38	18	100.0	0.0	0.0	0.0

and 2+ intensity in $\leq 30\%$ of cells were considered weakly positive. Tumors with 1+ staining intensity in $>70\%$ of cells, 2+ intensity in 31–70%, or 3+ intensity in $\leq 30\%$ were considered moderately positive. Tumors with 2+ intensity in $>70\%$ or 3+ intensity in $>30\%$ of cells were considered strongly positive.

Statistics. Statistical calculations were performed with JMP 14 software (SAS Institute Inc., NC, USA). Contingency tables and the chi²-test were performed to search for associations between pan-keratin and tumor phenotype. Survival curves were calculated according to Kaplan-Meier. The Log-Rank test was applied to detect significant differences between groups.

Results

Technical issues. A total of 13,501 (85%) of 15,940 tumor samples were interpretable. The remaining 2439 (15%)

samples were not analyzable due to the lack of unequivocal tumor cells or missing tissue spots on the TMA. For the normal tissue TMA, a sufficient number of samples was always interpretable per tissue to determine pan-keratin immunostaining.

Pan-keratin in normal tissues. A positive pan-keratin immunostaining was seen in virtually all normal epithelial and mesothelial cells. The most significant exception was the adrenal cortex, where only a fraction of cells, typically arranged in groups, fascicles or sheets, stained weakly to moderately positive. A somewhat lower, but still moderate to strong staining intensity than in most other epithelial cells was seen in hepatocytes, Langerhans islets in the pancreas, and pneumocytes of the lung. In lymph nodes, tonsil, spleen, and the thymus, a delicate fibrillar staining caused by fibroblastic reticulum cells was regularly seen, mainly in the interfollicular area. Occasional pan-keratin positive spindle shaped myofibroblasts occurred in

multiple organs, especially in case of degenerative or chronic inflammatory conditions. They were, for example, seen in the media of the aorta, muscular wall of the gallbladder, placental stroma, or in the ovary in the vicinity of a corpus luteum. Groups of spindle-shaped pan-keratin positive cells were also found in the myometrium. Pan-keratin immunostaining was absent in the testis, endothelial cells, the heart, striated muscle, muscular wall of the appendix, esophagus, stomach, ileum, colon, renal pelvis and urinary bladder, corpus spongiosum of the penis, ovarian stroma, fat, testis, neurohypophysis, cerebellum and cerebrum. Representative

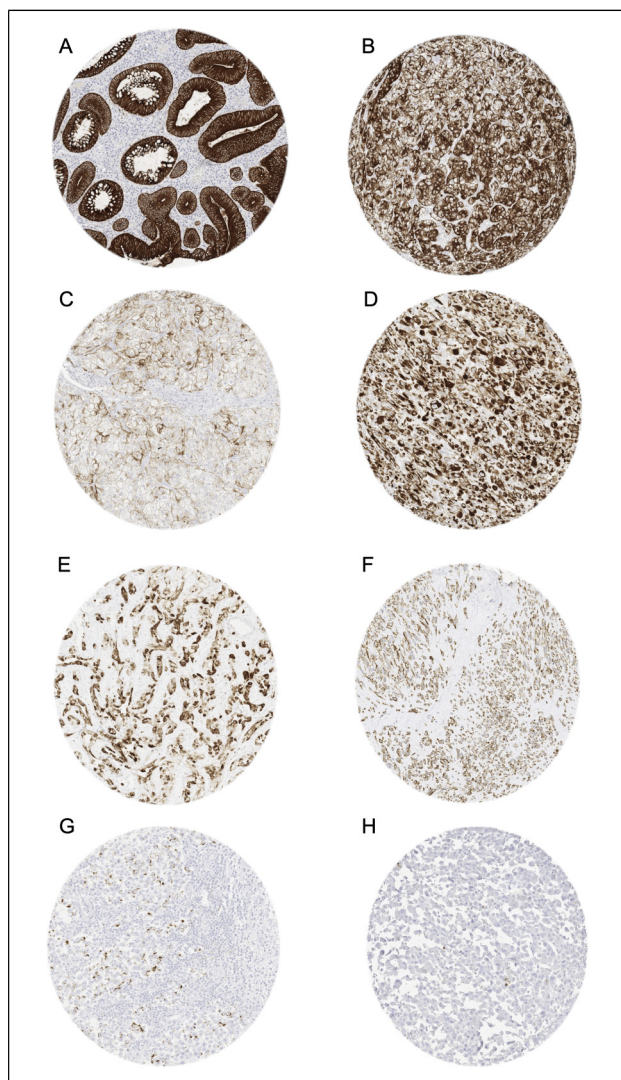


Figure 2. Pan-keratin immunostaining in tumors. The panels show a cytoplasmatic pan-keratin immunostaining of variable intensity in samples from a colorectal adenoma (A: strong staining), two clear cell renal cell carcinomas (B: strong; C: weak), a sarcoma NOS (D: strong), an angiosarcoma (E: strong), a gastrointestinal stromal tumor (GIST) (F: moderate), and a seminoma (G: weak). Pan-keratin immunostaining is lacking in an adrenocortical carcinoma (H).

images of pan-keratin positive normal tissues are shown in Figure 1.

Pan-keratin in tumors. A membranous and cytoplasmic pan-keratin immunostaining was observed in 11,323 (84%) of 13,501 analyzable tumors, including 79% with strong, 2.1% with moderate, and 2.6% with weak staining intensity. At least an occasional weak pan-keratin positivity could be detected in 101 of 121 (84%) different tumor types and tumor subtypes (Table 1). Among 75 epithelial tumor entities, the pan-keratin positivity rate was 100% in 50 (67%) and 98 – 99.9% in 12 categories (16%). These tumors included almost all adenocarcinomas,

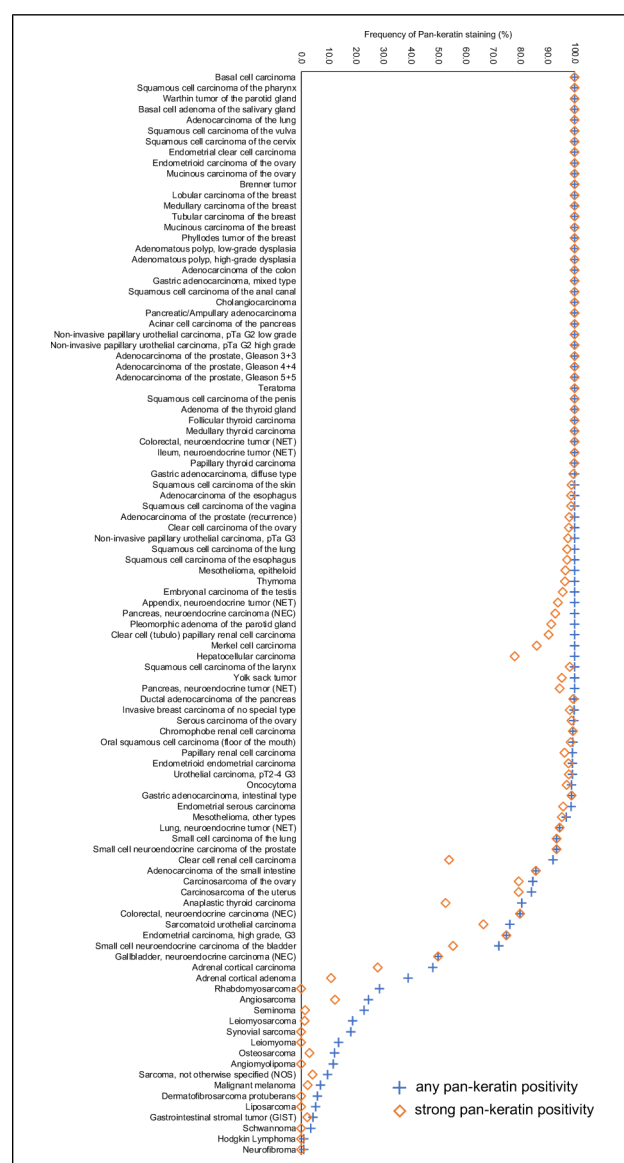


Figure 3. Ranking order of pan-keratin immunostaining in tumors. Both the frequency of positive tumors (blue cross) and the frequency of strongly positive tumors (orange rhombus) are shown.

Table 2. Pan-Keratin Immunostaining and Tumor Phenotype in Breast and Clear Cell Renal and Papillary Renal Cell Cancer.

			n	Pan-keratin IHC result				P
					negative (%)	weak (%)	moderate (%)	
Breast carcinoma of no special type	Primary Tumor	pT1	547	0.5	0.5	0.0	98.9	0.0023
		pT2	400	0.0	1.0	1.5	97.5	
		pT3-4	89	0.0	0.0	3.4	96.6	
	Grade	G1	171	0.6	0.6	0.0	98.8	0.0005
		G2	538	0.2	0.4	0.0	99.4	
		G3	366	0.3	1.1	2.7	95.9	
	Regional Lymph Nodes	pN0	444	0.0	0.7	0.9	98.4	0.7401
		pN1	217	0.0	0.5	0.9	98.6	
		pN2	72	0.0	0.0	0.0	100.0	
		pN3	50	0.0	0.0	0.0	100.0	
Clear cell renal cell carcinoma	HER2 status	negative	840	0.4	0.6	1.1	98.0	0.5544
		positive	114	0.0	0.0	0.9	99.1	
		negative	198	0.5	1.5	4.5	93.4	
		positive	713	0.1	0.3	0.1	99.4	
	PR status	negative	381	0.3	0.8	2.6	96.3	<0.0001
		positive	564	0.2	0.4	0.0	99.5	
		no	749	0.1	0.3	0.3	99.3	
		yes	133	0.8	2.3	6.0	91.0	
	Triple negative	no	236	7.6	17.8	21.2	53.4	0.1907
		yes	248	7.7	17.3	21.0	54.0	
Papillary renal cell carcinoma	ISUP grade	1	206	7.8	20.9	19.4	51.9	
		2	42	21.4	26.2	9.5	42.9	
		3	38	7.9	5.3	15.8	71.1	
		4	443	7.4	18.1	21.2	53.3	
	Fuhrmann grade	1	210	7.6	21.0	21.0	50.5	0.0049
		2	50	20.0	26.0	6.0	48.0	
		3	268	6.3	17.2	20.1	56.3	
		4	406	8.6	18.0	21.4	52.0	
	Thoenes grade	1	67	14.9	29.9	9.0	46.3	0.0183
		2	340	3.5	15.0	17.9	63.5	
		3	35	8.6	8.6	22.9	60.0	
Papillary renal cell carcinoma	UICC stage	3	91	14.3	24.2	17.6	44.0	
		4	74	13.5	14.9	21.6	50.0	
		1	446	4.9	17.0	17.9	60.1	
		2	76	10.5	19.7	26.3	43.4	
	Primary Tumor	3-4	214	15.0	22.4	21.0	41.6	<0.0001
		0	127	9.4	22.0	22.0	46.5	
		≥1	18	16.7	0.0	11.1	72.2	
	Regional Lymph Nodes	0	113	6.2	15.9	22.1	55.8	0.192
		≥1	76	15.8	14.5	22.4	47.4	
Papillary renal cell carcinoma	ISUP grade	1	40	0.0	0.0	2.5	97.5	0.933
		2	92	1.1	2.2	1.1	95.7	
		3	58	1.7	1.7	3.4	93.1	
		4	1	0.0	0.0	0.0	100.0	
	Fuhrmann grade	1	2	0.0	0.0	0.0	100.0	0.9965
		2	130	0.8	1.5	1.5	96.2	
		3	56	1.8	1.8	3.6	92.9	
		4	3	0.0	0.0	0.0	100.0	

(continued)

Table 2. (continued).

	n	Pan-keratin IHC result				P	
		negative (%)	weak (%)	moderate (%)	strong (%)		
Thoenes grade	1	49	0.0	0.0	2.0	98.0	0.664
	2	133	1.5	2.3	2.3	94.0	
	3	9	0.0	0.0	0.0	100.0	
UICC stage	1	104	0.0	1.0	0.0	99.0	0.0062
	2	18	0.0	0.0	5.6	94.4	
	3	5	20.0	0.0	40.0	40.0	
	4	12	0.0	0.0	0.0	100.0	
Primary Tumor	1	133	0.0	0.8	0.0	99.2	0.0007
	2	37	2.7	2.7	2.7	91.9	
	3-4	15	6.7	6.7	20.0	66.7	
Regional Lymph Nodes	0	19	0.0	0.0	5.3	94.7	0.423
	≥1	7	0.0	0.0	0.0	100.0	
Distant Metastasis	0	27	0.0	0.0	3.7	96.3	0.4935
	≥1	7	0.0	0.0	0.0	100.0	

squamous cell and urothelial carcinomas. Only 17 of 121 tumor entities (13%) had a pan-keratin positivity rate between 25% and 98%. This group mainly included tumors with mixed differentiation, endocrine/neuroendocrine tumors, renal cell carcinomas, adrenocortical tumors, and particularly poorly differentiated carcinoma subtypes (anaplastic, small cell, sarcomatoid). The tumors with a pan-keratin positivity in the range of 0.9%-25% included 15 tumor entities. Most of these were of mesenchymal origin and often showed a weaker staining than epithelial neoplasms. The 20 (17%) tumor entities that were always pan-keratin negative were all of mesenchymal and hemato-lymphatic origin. Representative images of pan-keratin positive tumors are shown in Figure 2. A graphical representation of a ranking order of pan-keratin positive tumors and the observed staining intensities in these tumors is given in Figure 3. These data also show, that most tumor entities with 90%-100% positive tumors showed a strong pan-keratin immunostaining while the staining intensity decreased in tumors entities with lower positivity rates. That significant pan-keratin staining can occur in sarcomas was also confirmed by using a second independent pan-keratin antibody (Supplementary Figure 1).

Pan-keratin immunostaining, tumor phenotype, and prognosis. The relationship between pan-keratin immunostaining and clinico-pathological data could be analyzed in breast and kidney cancer (Table 2). Reduced or absent pan-keratin immunostaining was associated with high UICC stage ($p = 0.001$), high Thoenes grade ($p = 0.0183$), high Fuhrman grade ($p = 0.0049$), advanced tumor stage ($p < 0.0001$) as well as lymph node metastasis ($p = 0.0114$) in clear cell renal

cell carcinomas, with high UICC stage ($p = 0.0062$) and advanced pT stage ($p = 0.0007$) in papillary renal cell carcinoma, and with advanced stage ($p = 0.0023$), high grade ($p = 0.0005$) as well as loss of estrogen receptor (ER) and progesterone receptor (PR) expression and a triple-negative status ($p < 0.0001$ each) in invasive breast carcinoma of no special type (NST). Despite a tendency towards shortened recurrence free (Figure 4a; $p = 0.1890$) and overall survival (Figure 4b, $p = 0.1234$) for pan-keratin negative clear cell renal cell carcinomas, this difference did not reach statistical significance. Reduced pan-keratin immunostaining was not statistically linked to poor outcome in NST (Figure 4c, $p = 0.2863$) but there were only 6 patients with reduced pan-keratin staining for which clinical follow-up data were available.

Discussion

The standardized analysis of 13,501 tumors provided a comprehensive overview on pan-keratin immunostaining in different tumor types. That the graphical representation of the frequencies of pan-keratin immunostaining among 121 different tumor entities resulted in an S-shaped curve reflects the fact that intense pan-keratin immunostaining is common in epithelial neoplasms while non-epithelial tumors are usually pan-keratin negative.

Among epithelial tumor entities, 50 of 75 (67%) showed Pan-keratin positivity in 100% of tumors and 12 (16%) were positive in ≥98% of tumors. These entities include virtually all important types of adenocarcinomas and squamous cell carcinomas. We assume that a fraction of the few negative tumors in these cancer types may be

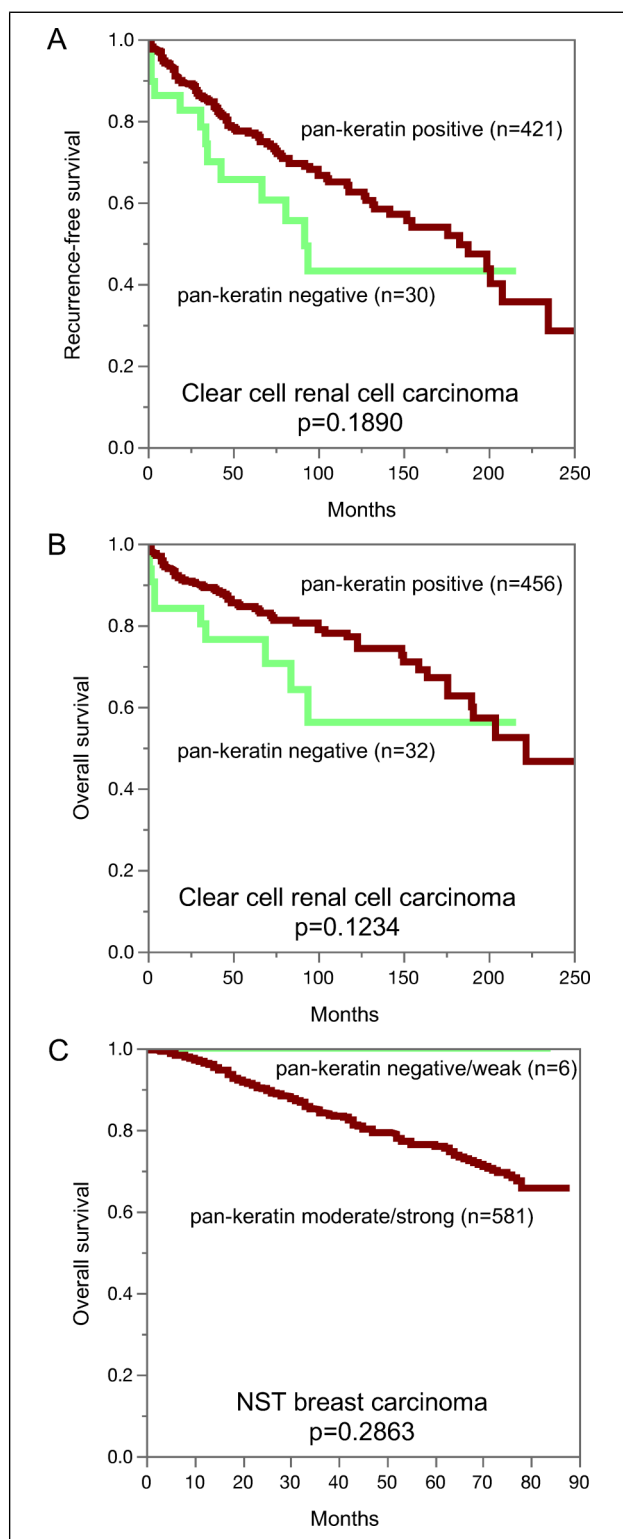


Figure 4. Pan-keratin immunostaining and recurrence-free survival (A) and overall survival (B) in clear cell renal cancer. Pan-keratin immunostaining in NST breast cancer and overall survival (C).

caused by technical issues. Some unexpected negative immunostaining results always occur in TMAs because not all tissues are properly fixed in all areas.²⁵ Unequal

immunostaining in tissues can result in an immunostaining gradient across a tissue block and can thus cause false negative immunostaining, if TMA cores are taken from areas with poor reactivity.²⁶ It is likely that – in at least a fraction of these tumors – some immunoreactive areas will be found if larger tissue samples, perhaps derived from different blocks, are analyzed.

The group of tumor entities with a pan-keratin positivity in 25% to 98% of analyzed tumors made up for only 17 (13%) of analyzed entities. Most of these tumors could be categorized into the following 5 groups: tumors with mixed differentiation, endocrine/neuroendocrine tumors, kidney tumors, adrenocortical tumors, and particularly poorly differentiated carcinoma subtypes. The group of tumors with mixed epithelial-mesenchymal differentiation includes carcinosarcoma of the uterus and the ovary, phyllodes tumor of the breast, teratoma of the testis, and malignant mesothelioma. In these tumors, epithelial but not mesenchymal tumor areas are pan-keratin positive. The pan-keratin TMA result therefore depends on whether epithelial components are present in the TMA spot or not. The rather low positivity rate in kidney cancers reflects the fact that these tumors have low cytokeratin levels and tend to express vimentin instead.^{27,28}

For adrenocortical, neuroendocrine and endocrine tumors, the intermediate positivity rate appears to mirror the rather low pan-keratin immunostaining in corresponding normal cells. Hepatocellular carcinoma, another tumor for which reduced cytokeratin has often been reported^{5,29,30} was always pan-keratin positive in this study, although staining was only weak or moderate in 22% of tumors.

Very poorly differentiated cancers, such as small cell and sarcomatoid cancers as well as anaplastic cancers of the thyroid, often showed lower pan-keratin immunostaining rates as compared to corresponding normal tissues and more differentiated tumors from these organs. This may reflect that a reduced expression of keratins is a feature of tumors dedifferentiation that can occur during cancer progression. This interpretation is also in line with our findings in kidney and breast carcinomas showing significant associations between reduced pan-keratin immunostaining and several unfavorable phenotypic tumor features. Other investigators had previously also described significant correlations between reduced expression of specific keratins^{31–34} or reduced pan-keratin immunostaining³⁵ and poor patient prognosis or unfavorable tumor phenotype in various tumor types. A reduced expression of keratins in tumors derived from keratin positive progenitor cells is likely to represent a feature of cellular dedifferentiation which regularly goes along with cancer progression. Our data also emphasize that pan-keratin immunostaining is not uncommon in mesenchymal tumors although the expression levels are usually lower in these neoplasms as compared to carcinomas. In this study, pan-keratin

immunostaining was observed in 13 mesenchymal tumor entities with highest rates in rhabdomyosarcomas (29%) and angiosarcomas (25%). These findings are in line with earlier studies describing keratin expression in 20%, 36%, 100% of rhabdomyosarcomas³⁶⁻³⁸ and in 20%, 33%, and 88% of angiosarcomas.^{19,20,39} Given the significant pan-keratin staining in the majority of cells is several sarcomas of different types, cytokeratin positivity – even if strong – should not automatically lead to a diagnosis of “sarcomatoid carcinoma”.

In summary, our data show that pan-keratin can consistently be detected in the vast majority of epithelial tumors but also identify renal cell, hepatocellular, adrenocortical and neuroendocrine neoplasms as tumors lacking pan-keratin immunostaining in a fraction of tumors. Moreover, pan-keratin immunostaining - usually at lower levels - can also occur in a broad range of mesenchymal tumors.

Acknowledgements

We are grateful to Melanie Witt, Inge Brandt, Maren Eisenberg, and Sünje Seekamp for excellent technical assistance.

Contributors

AM, RS, GS, CB: contributed to conception, design, data collection, data analysis and manuscript writing. NG, FV, ML, AML, EB, DH, CF, PL, RU, FJ, SM, TSC, DD: participated in pathology data analysis and data interpretation. TK, AHM collection of samples

AM, CB: immunohistochemistry analysis. RS, LH, MK, CHM: data analysis. AM, RS, GS, CB: study supervision. All authors agree to be accountable for the content of the work.

Data Availability Statement

All data generated or analyzed during this study are included in this published article

Declaration of Conflicting Interests

The author(s) declared the following potential conflicts of interest with respect to the research, authorship, and/or publication of this article: The Pan-keratin antibody clone MSVA-000R was received from MS Validated Antibodies GmbH (owned by a family member of GS).

Ethical Approval

The use of archived remnants of diagnostic tissues for TMA manufacturing, their analysis for research purposes, and use of patient data were according to local laws (HmbKHG, §12) and analysis had been approved by the local ethics committee (Ethics commission Hamburg, WF-049/09). All work has been carried out in compliance with the Helsinki Declaration.

Funding

The author(s) received no financial support for the research, authorship, and/or publication of this article.

Informed Consent

Not applicable, because this article does not contain any studies with human or animal subjects.

Trial Registration

Not applicable, because this article does not contain any clinical trials.

ORCID iDs

Ronald Simon  <https://orcid.org/0000-0003-0158-4258>
Eike Burandt  <https://orcid.org/0000-0002-5705-9084>

Supplemental Material

Supplemental material for this article is available online.

References

- Badzio A, Czapiewski P, Gorczynski A, et al. Prognostic value of broad-spectrum keratin clones AE1/AE3 and CAM5.2 in small cell lung cancer patients undergoing pulmonary resection. *Acta Biochim Pol.* Feb 22 2019;66(1):111-114. doi:10.18388/abp.2018_2773
- Sangoi AR, Fujiwara M, West RB, et al. Immunohistochemical distinction of primary adrenal cortical lesions from metastatic clear cell renal cell carcinoma: a study of 248 cases. *Am J Surg Pathol.* May 2011;35(5):678-686. doi:10.1097/PAS.0b013e3182152629
- Lau SK, Prakash S, Geller SA, Alsabeh R. Comparative immunohistochemical profile of hepatocellular carcinoma, cholangiocarcinoma, and metastatic adenocarcinoma. *Hum Pathol.* Dec 2002;33(12):1175-1181. doi:10.1053/hupa.2002.130104
- Cote RJ, Cordon-Cardo C, Reuter VE, Rosen PP. Immunopathology of adrenal and renal cortical tumors. Coordinated change in antigen expression is associated with neoplastic conversion in the adrenal cortex. *Am J Pathol.* May 1990;136(5):1077-1084.
- Christensen WN, Boitnott JK, Kuhajda FP. Immunoperoxidase staining as a diagnostic aid for hepatocellular carcinoma. *Mod Pathol.* Jan 1989;2(1):8-12.
- Wick MR, Cherwitz DL, McGlennen RC, Dehner LP. Adrenocortical carcinoma. An immunohistochemical comparison with renal cell carcinoma. *Am J Pathol.* Feb 1986;122(2):343-352.
- Lin XY, Liu Y, Zhang Y, Yu JH, Wang EH. The co-expression of cytokeratin and p63 in epithelioid angiosarcoma of the parotid gland: a diagnostic pitfall. *Diagn Pathol.* Sep 3 2012;7(1):118. doi:10.1186/1746-1596-7-118
- Miettinen M, Fetisch JF. Distribution of keratins in normal endothelial cells and a spectrum of vascular tumors: implications in tumor diagnosis. *Hum Pathol.* Sep 2000;31(9):1062-1067. doi:10.1053/hupa.2000.9843
- Gu M, Antonescu CR, Guiter G, Huvos AG, Ladanyi M, Zakowski MF. Cytokeratin immunoreactivity in Ewing's sarcoma: prevalence in 50 cases confirmed by molecular diagnostic studies. *Am J Surg Pathol.* Mar 2000;24(3):410-416. doi:10.1097/00000478-200003000-00010

10. Iwata J, Fletcher CD. Immunohistochemical detection of cytokeratin and epithelial membrane antigen in leiomyosarcoma: a systematic study of 100 cases. *Pathol Int.* Jan 2000;50(1):7-14. doi:10.1046/j.1440-1827.2000.01001.x
11. Meis-Kindblom JM, Kindblom LG. Angiosarcoma of soft tissue: a study of 80 cases. *Am J Surg Pathol.* Jun 1998;22(6):683-697. doi:10.1097/00000478-199806000-00005
12. Miettinen M. Immunoreactivity for cytokeratin and epithelial membrane antigen in leiomyosarcoma. *Arch Pathol Lab Med.* Jun 1988;112(6):637-640.
13. Lapinska JE, Chen L, Zhou M. Distinguishing clear cell renal cell carcinoma, retroperitoneal paraganglioma, and adrenal cortical lesions on limited biopsy material: utility of immunohistochemical markers. *Appl Immunohistochem Mol Morphol.* Oct 2010;18(5):414-421. doi:10.1097/PAI.0b013e3181ddf7b9
14. Pinkus GS, Etheridge CL, O'Connor EM. Are keratin proteins a better tumor marker than epithelial membrane antigen? A comparative immunohistochemical study of various paraffin-embedded neoplasms using monoclonal and polyclonal antibodies. *Am J Clin Pathol.* Mar 1986;85(3):269-277. doi:10.1093/ajcp/85.3.269
15. He H, Trpkov K, Martinek P, et al. "High-grade oncocytic renal tumor": morphologic, immunohistochemical, and molecular genetic study of 14 cases. *Virchows Arch.* Dec 2018;473(6):725-738. doi:10.1007/s00428-018-2456-4
16. Hayes M, Peckova K, Martinek P, et al. Molecular-genetic analysis is essential for accurate classification of renal carcinoma resembling Xp11.2 translocation carcinoma. *Virchows Arch.* Mar 2015;466(3):313-322. doi:10.1007/s00428-014-1702-7
17. Al-Obaidy KI, Eble JN, Cheng L, et al. Papillary renal neoplasm with reverse polarity: a morphologic, immunohistochemical, and molecular study. *Am J Surg Pathol.* Aug 2019;43(8):1099-1111. doi:10.1097/PAS.0000000000001288
18. Hes O, Brunelli M, Michal M, et al. Oncocytic papillary renal cell carcinoma: a clinicopathologic, immunohistochemical, ultrastructural, and interphase cytogenetic study of 12 cases. *Ann Diagn Pathol.* Jun 2006;10(3):133-139. doi:10.1016/j.anndiagpath.2005.12.002
19. Nakashima Y, Inamura K, Ninomiya H, et al. Frequent expression of conventional endothelial markers in pleural mesothelioma: usefulness of claudin-5 as well as combined traditional markers to distinguish mesothelioma from angiosarcoma. *Lung Cancer.* Oct 2020;148:20-27. doi:10.1016/j.lungcan.2020.07.029
20. Allison KH, Yoder BJ, Bronner MP, Goldblum JR, Rubin BP. Angiosarcoma involving the gastrointestinal tract: a series of primary and metastatic cases. *Am J Surg Pathol.* Mar 2004;28(3):298-307. doi:10.1097/00000478-20040300-00002
21. Abeler VM, Nenodovic M. Diagnostic immunohistochemistry in uterine sarcomas: a study of 397 cases. *Int J Gynecol Pathol.* May 2011;30(3):236-243. doi:10.1097/PGP.0b013e318200caff
22. Yang J, Eddy JA, Pan Y, et al. Integrated proteomics and genomics analysis reveals a novel mesenchymal to epithelial reverting transition in leiomyosarcoma through regulation of slug. *Mol Cell Proteomics.* Nov 2010;9(11):2405-2413. doi:10.1074/mcp.M110.000240
23. Dancau AM, Simon R, Mirlacher M, Sauter G. Tissue microarrays. *Methods Mol Biol.* 2016;1381:53-65. doi:10.1007/978-1-4939-3204-7_3
24. Kononen J, Bubendorf L, Kallioniemi A, et al. Tissue microarrays for high-throughput molecular profiling of tumor specimens. *Nat Med.* Jul 1998;4(7):844-847. doi:10.1038/nm0798-844
25. Tapia C, Schraml P, Simon R, et al. HER2 Analysis in breast cancer: reduced immunoreactivity in FISH non-informative cancer biopsies. *Int J Oncol.* Dec 2004;25(6):1551-1557.
26. Fraune C, Simon R, Huber-Magg C, et al. MMR deficiency in urothelial carcinoma of the bladder presents with temporal and spatial homogeneity throughout the tumor mass. *Urol Oncol.* May 2020;38(5):488-495. doi:10.1016/j.urolonc.2019.12.012
27. Skinnider BF, Folpe AL, Hennigar RA, et al. Distribution of cytokeratins and vimentin in adult renal neoplasms and normal renal tissue: potential utility of a cytokeratin antibody panel in the differential diagnosis of renal tumors. *Am J Surg Pathol.* Jun 2005;29(6):747-754. doi:10.1097/01.pas.0000163362.78475.63
28. Alexa A, Baderca F, Lighezan R, Izvernariu D, Raica M. The diagnostic value of cytokeratins expression in the renal parenchyma tumors. *Rom J Morphol Embryol.* 2010;51(1):27-35.
29. Van Eyken P, Sciot R, Desmet VJ. Immunocytochemistry of cytokeratins in primary human liver tumors. *APMIS Suppl.* 1991;23:77-85.
30. Van Eyken P, Sciot R, Paterson A, Callea F, Kew MC, Desmet VJ. Cytokeratin expression in hepatocellular carcinoma: an immunohistochemical study. *Hum Pathol.* May 1988;19(5):562-568. doi:10.1016/s0046-8177(88)80205-3
31. Pandey S, Soland TM, Bjerkli IH, et al. Combined loss of expression of involucrin and cytokeratin 13 is associated with poor prognosis in squamous cell carcinoma of mobile tongue. *Head Neck.* Nov 2021;43(11):3374-3385. doi:10.1002/hed.26826
32. Menz A, Bauer R, Kluth M, et al. Diagnostic and prognostic impact of cytokeratin 19 expression analysis in human tumors: a tissue microarray study of 13,172 tumors. *Hum Pathol.* Sep 2021;115:19-36. doi:10.1016/j.humpath.2021.05.012
33. Menz A, Weitbrecht T, Gorbokon N, et al. Diagnostic and prognostic impact of cytokeratin 18 expression in human tumors: a tissue microarray study on 11,952 tumors. *Mol Med.* Feb 15 2021;27(1):16. doi:10.1186/s10020-021-00274-7
34. Vora HH, Patel NA, Rajvik KN, et al. Cytokeratin and vimentin expression in breast cancer. *Int J Biol Markers.* Jan-Mar 2009;24(1):38-46. doi:10.5301/jbm.2009.4965
35. Rajkovic N, Li X, Plataniotis KN, Kanjer K, Radulovic M, Milosevic NT. The pan-cytokeratin staining intensity and fractal computational analysis of breast tumor malignant growth patterns prognosticate the occurrence of distant metastasis. *Front Oncol.* 2018;8:348. doi:10.3389/fonc.2018.00348
36. Le Loarer F, Cleven AHG, Bouvier C, et al. A subset of epithelioid and spindle cell rhabdomyosarcomas is associated

- with TFCP2 fusions and common ALK upregulation. *Mod Pathol.* Mar 2020;33(3):404-419. doi:10.1038/s41379-019-0323-8
37. Thompson LDR, Jo VY, Agaimy A, et al. Sinonasal tract alveolar rhabdomyosarcoma in adults: a clinicopathologic and immunophenotypic study of fifty-two cases with emphasis on epithelial immunoreactivity. *Head Neck Pathol.* Jun 2018;12(2):181-192. doi:10.1007/s12105-017-0851-9
38. Stock N, Chibon F, Binh MB, et al. Adult-type rhabdomyosarcoma: analysis of 57 cases with clinicopathologic description, identification of 3 morphologic patterns and prognosis. *Am J Surg Pathol.* Dec 2009;33(12):1850-1859. doi:10.1097/PAS.0b013e3181be6209
39. Matoso A, Epstein JI. Epithelioid angiosarcoma of the bladder: a series of 9 cases. *Am J Surg Pathol.* Oct 2015;39(10):1377-1382. doi:10.1097/PAS.0000000000000444